

The Oort spike modification due to non-gravitational effects

Małgorzata Królikowska*

Space Research Centre of the Polish Academy of Sciences
Bartycka 18A, 00-716, Warsaw, Poland

July 23, 2018

Abstract

This is the third of a series of papers on investigating the non-gravitational effects in the motion of long-period comets. The influence of the non-gravitational effects on the original and future orbital elements, and in particular on reciprocals of semimajor axes is analyzed. The new orbit determinations were performed in a homogenous way using the basic collection of 50 nearly-parabolic comets of first class orbits. The data consist of 23 hypothetically hyperbolic comets (sample I), 8 Oort spike comets (sample II), and 19 'old' comets (sample III). The original and future reciprocals of semimajor axes for each comet were calculated for strictly gravitational case and the non-gravitational case in a fully consistent way. Clear shift of the original reciprocals of semimajor axes toward the more elliptical orbits is demonstrated. The average values of the original and future energy changes due to the non-gravitational acceleration are derived for each of three samples independently. Omission of the NG effects significantly affects the position and width of the Oort spike. The shift of the Oort spike position from the standard $1/a_{\text{ori}}$ value of $2-4 \cdot 10^{-5} \text{ AU}^{-1}$ to the value greater than $5.5 \cdot 10^{-5} \text{ AU}^{-1}$ is discussed.

1 Introduction

More than half century ago Oort (1950) postulated that at distances of tens of thousands AU existed roughly spherical cloud of comets. He has built his famous idea on just 19 well determined cometary orbits. This classical vision of Oort cloud remains still valid on the basis of almost four hundred orbits of nearly-parabolic comets discovered up to now (Marsden and Williams Catalogue of Cometary Orbits, (Marsden & Williams, 2005), hereafter MW Catalogue)¹. Almost 30% of long-period (LP) comets have $E_{\text{ori}} \equiv 1/a_{\text{ori}} < 10^{-4} \text{ AU}^{-1}$ where about one fourth of them have negative E_{ori} . However, recent determinations of the typical E_{ori} gave significantly smaller values than original indicated by Oort. Oort estimated that most of nearly parabolic comets have semimajor axes of about 25–75 thousands AU.

The median semimajor axis of the 109 comets with the first quality orbits and $0 < E_{\text{ori}} < 10^{-4} \text{ AU}^{-1}$ selected from the MW Catalogue is 27 800 AU where all orbits are strictly gravitational. If all available non-gravitational (NG) orbits of $0 < E_{\text{ori}} < 10^{-4} \text{ AU}^{-1}$ are used the sample increases to 120 comets and the median semimajor axis declines to 26 000 AU. This result strongly suggests that taking the NG effects into account may reduce the Oort Cloud distance from the Sun significantly below 50 000 AU.

In the above estimates the comets with a negative value of the binding energy were excluded. These objects could be interstellar intruders passing through the inner solar system. However, the modern estimates of the expected rate for extrasolar comet detection give at most a few on average every 450 yrs (Sen & Rana, 1993; Hughes, 1991). Thus the majority of 'hyperbolic' comets have to have local origin. This discrepancy between observations and theoretical expectations disappears when the NG effects are included for orbit determination (Marsden et al. (1973; 1978), Królikowska (2001)(Paper I) (2004)(Paper II)). It is due to a fact, that NG forces make 'hyperbolic' and elliptical osculating orbits on the average less eccentric than in the case of purely gravitational motion. Consequently, omission of the NG effects may significantly affect the position and width of the Oort spike. It means also that the apparent inner edge of the Oort cloud should be shifted towards the more positive $1/a_{\text{ori}}$. In the present paper I try to give quantitative estimates for the magnitude of these shifts.

In Paper I the sample of 33 comets with negative value of reciprocals of original semimajor axis were analyzed and for 16 of them the NG-effects could be determined. It was shown that for 14 of these 16 comets the incoming barycentric orbits changed from hyperbolic to ecliptic when the NG effects were included. In sections 2 and 3 of the present paper the analysis of the NG effects for the almost complete sample of comets that have the catalogue

*email: mkr@cbk.waw.pl

¹Almost all orbits of nearly parabolic comets are derived as purely gravitational

Table 1: The samples of the investigated LP comets with first quality orbits

| Comets | designation | criterion | Number of comets |
|--|-------------|--|------------------|
| Basic samples (contain comets with the detectable NG effects) | | | |
| 'new' | I | $1/a_{\text{ori}} < 10^{-5} \text{ AU}^{-1}$ | 23 |
| Oort spike | II | $10^{-5} \text{ AU}^{-1} < 1/a_{\text{ori}} < 10^{-4} \text{ AU}^{-1}$ | 8 |
| 'old' | III | $1/a_{\text{ori}} > 10^{-4} \text{ AU}^{-1}$ | 19 |
| Global samples constructed directly from the MW Catalogue; | | | |
| contain LP comets with aphelions $Q > 250 \text{ AU}$ | | | |
| 'new'+Oort spike | A | $1/a_{\text{ori}} < 10^{-4} \text{ AU}^{-1}$ | 131 |
| 'old' | B | $1/a_{\text{ori}} > 10^{-4} \text{ AU}^{-1}$ | 131 |
| Corrected global samples | | | |
| contain LP comets with aphelions $Q > 250 \text{ AU}$ | | | |
| 'new'+Oort spike | AA | $1/a_{\text{ori}} < 10^{-4} \text{ AU}^{-1}$ | 144-7 |
| 'old' | BB | $1/a_{\text{ori}} > 10^{-4} \text{ AU}^{-1}$ | 142+7 |

value² of $1/a_{\text{ori}} < 10^{-5} \text{ AU}^{-1}$ is performed. For those comets the term 'dynamically new' (in short 'new') is applied, while comets with $10^{-5} \text{ AU}^{-1} < 1/a_{\text{ori}} < 10^{-4} \text{ AU}^{-1}$ are defined as the 'Oort spike' comets. This differentiation between 'new' and 'Oort spike' comets, however, does not imply that the Oort spike comets cannot be dynamically new objects. In fact, simulations by Dybczynski (2005) have shown that the value of $4 \cdot 10^{-5} \text{ AU}^{-1}$ suggested previously by Marsden and Sekanina (1973) is the most appropriate for definition of dynamically new comets. In Section 4 two other samples of LP comets with NG effects have been constructed. The first sample contains comets with the catalogue orbit inside the Oort spike (8 objects), the second – comets with catalogue $1/a_{\text{ori}} > 10^{-4} \text{ AU}^{-1}$ (19 objects). It is important to stress that the NG effects were derived simultaneously with osculating orbital elements from the positional data taken near perihelion passage and were then consistently applied to determine the original/future orbits and original/future reciprocals of semimajor axis. The variations of the original and future energy due to the NG effects are widely discussed in Section 6, where the average values of differences between the original orbital energies derived from NG orbit and strictly gravitational orbit, $\Delta E_{\text{ori}} = 1/a_{\text{ori,NG}} - 1/a_{\text{ori,GR}}$, were determined separately for all three basic samples. These average values of ΔE_{ori} allow to correct the observed Oort spike for the NG-effects (section 7).

Modern simulations of the Oort Cloud evolution predict that the observed sample of new comets that reach the inner solar system is biased to objects with the semimajor axes greater than 20 000–30 000 AU because of the 'Jupiter barrier'. New comets must have decreased their perihelion distances from more than 10 AU to less than 3 AU in one orbital period. Otherwise, they had a chance to encounter Jupiter and/or Saturn during their earlier evolution, which would remove them from the Oort spike. Heisler (1990) has derived that the binding energies of Oort spike comets are peaked at $E_{\text{ori}} = 3.5 \cdot 10^{-5} \text{ AU}^{-1}$ ($a \sim 29 000 \text{ AU}$), assuming a local density of $0.185 \text{ M}_{\odot}/\text{pc}^3$. Taking currently accepted value of $0.1 \text{ M}_{\odot}/\text{pc}^3$ for local density, Levison et al. (2001) argued that the maximum should be rather at $\sim 34 000 \text{ AU}$, whereas the inner edge of the outer Oort cloud – at $\sim 28 000 \text{ AU}$. Thus, one should notice some discrepancy between the theoretical predictions and apparent inner edge at 20 000 AU. However, both the theoretical calculations and orbit determinations do not include the NG-effects. Hence it is open question if this discrepancy is real (Rickman, 2004).

2 Sample of hypothetic 'hyperbolic' comets

The MW Catalogue contains 404 'single-apparitions' nearly-parabolic comets of the first and second quality orbits in the MW Catalogue with aphelion greater than 250 AU. Among them 29 comets have the NG orbits, and these objects are analyzed separately.

To calculate the original and future reciprocals of the semimajor axes, each of 375 (404 – 29) comets were followed from their position at a given epoch backwards (incoming orbit before entry into the planetary system) and forwards (outgoing orbit after planetary perturbations) until the comet reached a distance of 250 AU from the Sun. The equations of motion have been integrated in barycentric coordinates using the recurrent power series method (Sitarzki (1989; 2002)) taking into account the perturbations by all nine planets. All the numerical calculations presented here are based on the Warsaw ephemeris DE405/WAW, i.e. the numerical Solar System ephemeris consistent to high accuracy with the JPL ephemeris DE405 (Sitarzki, 2002).

The sample of 44 comets with original value of energy $E_0 \equiv 1/a_{\text{ori}} < 10^{-5} \text{ AU}^{-1}$ was extracted from the 375 sets of the orbital elements taken from the MW Catalogue (2005). The derived values of $1/a_{\text{ori}}$ were generally very similar to those given in the MW Catalogue. However, three comets in part (i) of Table 6 have catalogue values of $1/a_{\text{ori}}$ greater than 10^{-5} AU^{-1} (C/1978 R3, C/1987 W3, C/2002 A3).

²By catalogue value I mean the value given in MW Catalogue of Cometary Orbits, 2005

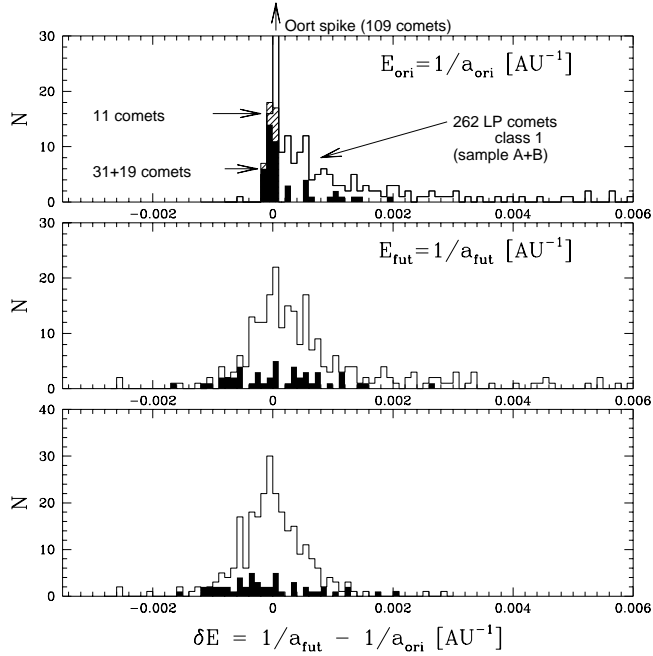


Figure 1: Distributions of cometary energies, $E_{\text{ori}} \equiv 1/a_{\text{ori}}$ (top panel), and $E_{\text{fut}} \equiv 1/a_{\text{fut}}$ (middle panel), $\delta E \equiv 1/a_{\text{fut}} - 1/a_{\text{ori}}$ (bottom panel). The filled histograms show the respective energy distributions derived for strictly gravitational orbits for all of the investigated comets (50 objects from all three samples: I+II+III; Table 1). The shaded histogram drawn in the top panel represents the 11 comets with $E_{\text{ori}} < 10^{-5} \text{ AU}^{-1}$, where the NG-effects were indeterminable (part (i) of Table 6; sample AA). The solid line histograms represent global distributions of all comets with first quality orbits and aphelions $Q > 250 \text{ AU}$ taken from MW Catalogue (sample A+B, Table 1)

Among these 44 objects, one is the secondary component of the splitting event (C/1996 J1A). It is obvious that original orbits, in particular the value of $1/a_{\text{ori}}$, would be unreliable for this fragment. The leading component of this splitting is included (part (i) of Tables 6). The observations for the three comets (C/1849 G2, C/1906 B1, C/1959 O1) were not available. Four recently discovered comets (C/2003 T3, C/2005 B1, C/2005 G1 and C/2005 K1) are still potentially observable and were not taken into account. The resulting sample of 36 comets was supplemented by eleven comets with NG-orbits in the MW Catalogue for which $1/a_{\text{ori}} < 10^{-5} \text{ AU}^{-1}$ were obtained for strictly gravitational orbits determined directly from observations.

Thus, the new orbit determination was performed for 47 objects of the sample of 'dynamically new' comets, where 34 have the first class orbits. Seven comets in this sample (C/1959 Y1, C/1986 P1A, C/1990 K1 C/1993 A1, C/1995 Y1, C/1996 E1, C/1998 P1) were previously analyzed in Paper II and their osculating orbits for strictly gravitational model and standard NG-model presented there are incorporated into the present data. Of the remaining 40 objects, 27 comets have been investigated in Paper I. In the present paper for eight of them the observational material has been significantly extended. I additionally collected all observations available in the literature for six comets that were discovered at the end of XIXth century. For the eight comets observed during the period 1900-1950 the analysis was based using the data collected in Warsaw in cooperation with the Slovakian group at the Astronomical Institute from Bratislava and Tatranska Lomnica. Generally, the positional data used for the orbit determination in the present work are more complete than the data described in the MW Catalogue. The observational arcs and number of observations taken for the strictly gravitational and NG orbital fitting to the positional data are collected in Table 6 (parts (i) and (ii)) for all the comets with the first class orbits (34 objects) as well as for six comets with the second class orbits and with determinable NG effects (6 objects). Seven comets with the second class orbits have indeterminable NG effects and these objects are not presented in Table 6.

The original and future reciprocals of semimajor axis obtained from the new orbit determinations of these 40 'new' comets are given in parts (i) and (ii) of Table 6 (columns 7-10). The basic sample I was constructed from the 'new' comets having first quality orbits and the detectable NG effects (column 6 of Table 6).

3 Comparison between new and previous orbit determinations

New determinations of osculating orbits and original and future reciprocals of semimajor axis (Table 6, columns 6-9) differ in a few cases from those given in Paper I (Tables 1 and 2 therein) due to three reasons.

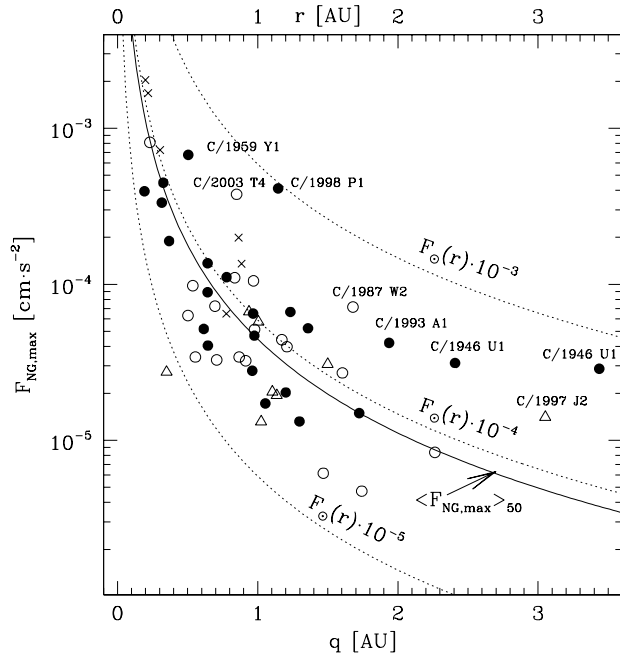


Figure 2: Maximum values of the NG forces $F_{NG,max} = A_1 \cdot g(r = q)$ vs. perihelion distance, q , derived for the investigated LP comets. Full circles, open triangles, and open circles show maximum values of the NG-forces for the sample I, II, and III, respectively. The crosses represent six comets with second quality class orbits given in part(i) of Table 6. The dotted curves represent the 10^{-3} , 10^{-4} , 10^{-5} of the solar gravitational acceleration $F_{\odot}(r)$, respectively, while the solid curve shows the mean value of $F_{NG,max}$ derived from the sample I+II+III

First, the observational material for several comets is more complete than in Paper I. Second, I have applied the different selection procedure that was successfully verified using the long-period comets with NG-effects (Paper II), where the pre-perihelion and post-perihelion observations were selected separately.

This new approach and larger observational data have allowed to determine the NG-effects for six comets listed in Paper I among objects with the indeterminable NG-effects (C/1899 E1, C/1952 W1, C/1892 Q1, C/1996 J1B, C/1997 BA6, C/1997 J2). Moreover, residuals for another six comets investigated also in Paper I are greater than those given there. In all cases the new selection procedure removes smaller sets of positional observations in rectascension or/and in declination than the method applied in Paper I.

Finally, the present numerical calculations are based on the Solar System ephemeris DE405/WAW, whereas the results given in Paper I were based on the older one. For more detailed discussion see Paper II.

4 Two other samples of comets with detectable NG effects

I have constructed two other samples of comets with the detectable NG-effects and the first quality orbits: Oort spike comets ($10^{-5} \text{ AU}^{-1} < E_{\text{ori}} < 10^{-4} \text{ AU}^{-1}$; 8 objects) and 'old' comets ($E_{\text{ori}} > 10^{-4} \text{ AU}^{-1}$; 19 comets). The observational material of both samples and the original and future reciprocals of semimajor axis are given in Table 6. In the present calculations I have also used the positional data, the NG solutions as well as the original and future orbits for 12 of 19 LP comets given in the Paper II (see Table 1 and 2 therein).

Three samples of comets with the detectable NG effects are described in Table 1, whereas the distributions of $1/a_{\text{ori}}$, $1/a_{\text{fut}}$ and $\Delta E = 1/a_{\text{fut}} - 1/a_{\text{ori}}$ are shown in Fig. 1.

5 Non-gravitational effects of cometary outgassing

The detailed discussion on modeling of the NG effects in LP comets was given in Paper II. Since one of the objectives of present investigation is to construct the samples of homogeneously derived NG orbits, the standard function $g(r)$ proposed by Marsden et al. (1973) was adopted here for all the comets except comet C/1959 Y1 Burnham, for which it is evident that the asymmetric function $g(r(t - \tau))$ much better represents the comet NG motion (Paper II). Thus, the three NG parameters A_1 , A_2 and A_3 were derived simultaneously with six orbital elements from the

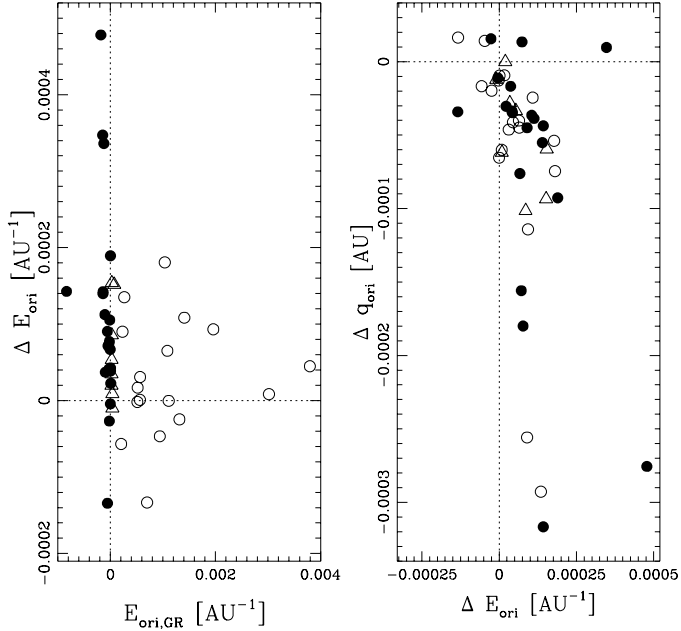


Figure 3: The original energy changes $\Delta E_{\text{ori}} = E_{\text{ori,NG}} - E_{\text{ori,GR}}$ as a function of the original energy $E_{\text{ori,NG}}$ (left panel) and relation between the perihelion distance variations, Δq_{ori} and ΔE_{ori} (right panel). Full circles, open triangles, and open circles show values for the sample I, II, and III, respectively.

orbital motion of each comet by assuming that the NG acceleration is given by equation

$$F_i = A_i \cdot g(r), \quad A_i = \text{const}$$

where $i = 1, 2, 3$ refer to the radial, transverse and normal components, respectively.

The investigated cometary samples I+II+III taken together contain 50 comets with determinable NG effects. It is well known that the actual amplitude of the NG forces is typically at least 10 times greater for LP comets than for the short period comets. Using the sample of 23 short-period comets and 7 LP comets, Marsden et al. (1973) have obtained that the actual magnitude of the NG forces is typically about 10^{-5} times the solar attraction at 1 AU for the short-period comets and $(1-2) \cdot 10^{-4}$ of the solar attraction for the LP comets. In Paper II the average value of $\langle F_{\text{NG,max}}/F_{\odot} \rangle = 1.5 \cdot 10^{-4}$ was derived for the sample of 19 LP comets containing 7 comets with $E_0 < 10^{-4} \text{ AU}^{-1}$ and 12 comets with $E_0 > 10^{-4} \text{ AU}^{-1}$. The results for investigated LP comets are given in column 3 of Table 2. The maxima of NG forces, $F_{\text{NG,max}}$, as a function of the perihelion distance, q , are shown in Fig. 2. The average value of the NG forces estimated from the whole sample of 50 comets $\langle F_{\text{NG,max}}/F_{\odot} \rangle = 7.6 \cdot 10^{-5}$, thus it is almost two times lower than previously derived in Paper II (using the sample of 19 LP comets).

6 Variations of original and future energy due to NG effects

Variations of the original energy, $\Delta E_{\text{ori}} = 1/a_{\text{ori,NG}} - 1/a_{\text{ori,GR}}$, as a function of $1/a_{\text{ori,GR}}$ and as a function of $\Delta q_{\text{ori}} = q_{\text{ori,NG}} - q_{\text{ori,GR}}$ are displayed in Fig 3.

Among 23 comets of the sample I (full circles in Fig. 3) four objects have negative ΔE_{ori} ; one such object is in the sample II (open triangles), and six in the sample III (open circles). Thus 11 of 50 comets with detectable NG-effects have original orbits more hyperbolic than their strictly gravitational orbits are. One can see in Fig. 3 that the values of ΔE_{ori} are significantly more spread for the sample I than for the samples II and III. Fig. 3 also does not reveal any significant correlations between ΔE_{ori} and Δq_{ori} (top panel). The values of Δq_{ori} span a range $-829 \cdot 10^{-6} \text{ AU} < \Delta q_{\text{ori}} < +16 \cdot 10^{-6} \text{ AU}$, excluding extremely positive value of $\Delta q_{\text{ori}} = 9860 \cdot 10^{-6} \text{ AU}$ for C/1997 BA6. Only 6 of 50 comets have positive Δq_{ori} . The median values of Δq_{ori} for three basic samples are very similar and amount to about $-40 \cdot 10^{-6} \text{ AU}$. Thus, it is evident that nearly parabolic comets have systematically smaller q_{ori} and more positive E_{ori} due to the NG-forces. The respective relations for the future orbits between energy and perihelion changes, and energy and energy variations are shown in Fig 5. The range of ΔE_{fut} is similar to the incoming orbits ($-160 \cdot 10^{-6} \text{ AU}^{-1} < \Delta E_{\text{fut}} < +600 \cdot 10^{-6} \text{ AU}^{-1}$) and the systematic trend to more elliptical

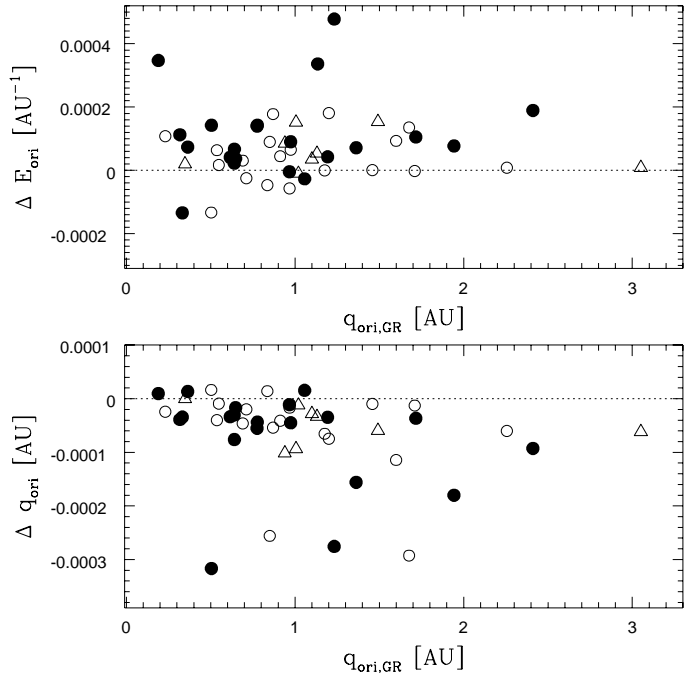


Figure 4: The original energy changes ΔE_{ori} and perihelion distance variations, Δq_{ori} as a function of the perihelion distance. Full circles, open triangles, and open circles show values for the sample I, II, and III, respectively.

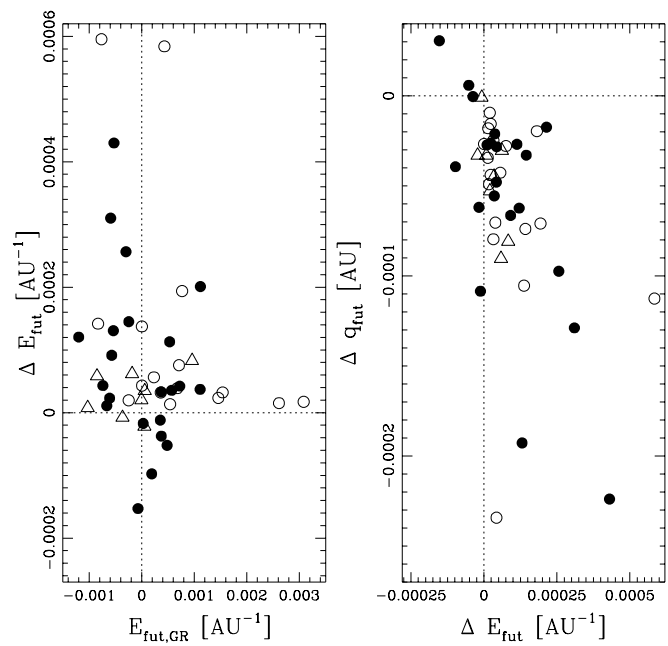


Figure 5: The same as in Fig. 3 for future energy changes $\Delta E_{\text{fut}} = E_{\text{fut,NG}} - E_{\text{fut,GR}}$ and future perihelion changes Δq_{fut}

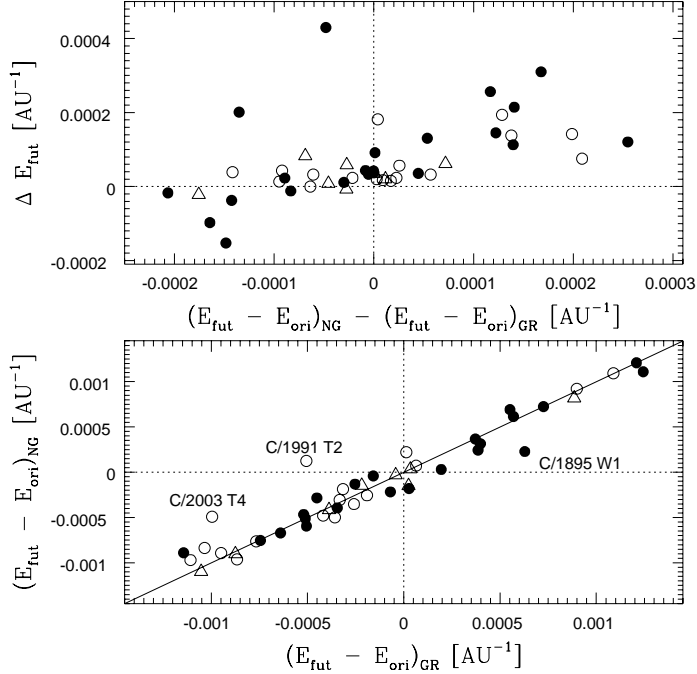


Figure 6: Bottom panel: Comparison between energy changes during the comet crossing through the Solar System for the non-gravitational and strictly gravitational case. Points are coded as in Figs 3–5. Top panel: Changes between the non-gravitational and strictly gravitational case shown in the plot $\Delta(E_{\text{fut}} - E_{\text{ori}})$ vs ΔE_{fut} .

Table 2: Two models derived for modification of $E_{\text{ori}} = a_{\text{ori}}^{-1}$ due to the NG effects. Model M1 is based on the median values of $\Delta E_{\text{ori}} = E_{\text{ori,NG}} - E_{\text{ori,GR}}$ and median values of $\Delta E_{\text{fut}} = E_{\text{fut,NG}} - E_{\text{fut,GR}}$ (columns 4–5), whereas Model M2 – on the average values of $\langle \Delta E_{\text{ori}} \rangle$, and $\langle \Delta E_{\text{fut}} \rangle$, (columns 6–7). The asterisk * denotes that two comets (C/1991 T2, C/2003 T4) with extremely large ΔE_{fut} value of about $600 \cdot 10^{-6} \text{ AU}^{-1}$ were excluded. The ranges of ΔE_{ori} and ΔE_{fut} are shown in columns 8 and 9, respectively. In column 3 the mean values of the NG-effects in perihelions, $\langle F_{\text{NG,max}}/F_{\odot} \rangle$, are given.

| Models used for Oort spike : | Model M1 | | Model M2 | | Range of | |
|------------------------------|-----------------|---|-------------------------|-------------------------|-------------------------|-------------------------|
| | Median value of | Mean value of | Median value of | Mean value of | | |
| Sample | Number | $\langle F_{\text{NG,max}}/F_{\odot} \rangle$ | ΔE_{ori} | ΔE_{fut} | ΔE_{ori} | ΔE_{fut} |
| | | | | | | |
| | | | | | | |
| I | 23 | 9.3 | 73.60 | 42.34 | 99.54 | 81.26 |
| II | 8 | 5.3 | 44.22 | 27.58 | 62.30 | 20.61 |
| III | 19 | 6.9 | 30.77 | 32.39* | 39.58 | 61.54* |
| I+II | 31 | 8.0 | 66.87 | 37.16 | 89.93 | 67.93 |
| I+II+III | 50 | 7.6 | 58.74 | 36.41* | 72.62 | 65.66* |
| | | | | | | |
| | | | | | | |

Table 3: The average values of the original energy, $\langle E_{\text{ori}} \rangle$ of strictly gravitational orbit (column 3) and the NG orbit (column 5) for comets of detectable NG effects binned according to their q values.

| Sample I+II, number of comets : 31 (open circles and triangles in Fig. 7) | | | | | |
|--|--------|------------------------------------|----------------------------------|------------------------------------|----------------------------------|
| range of q | number | strictly gravitational orbits | | NG orbits | |
| | | $\langle 1/a_{\text{ori}} \rangle$ | $\langle q_{\text{ori}} \rangle$ | $\langle 1/a_{\text{ori}} \rangle$ | $\langle q_{\text{ori}} \rangle$ |
| 0.00–0.50 | 5 | -0.00006257 | 0.3103 | 0.00002117 | 0.3103 |
| 0.50–1.00 | 10 | -0.00004255 | 0.7665 | 0.00002478 | 0.7665 |
| 1.00–3.10 | 16 | -0.00001118 | 1.5985 | 0.00009481 | 1.5990 |
| all | 31 | -0.00002959 | 1.1223 | 0.00006034 | 1.1226 |

| Sample III, number of comets : 19 (open squares in Fig. 7) | | | | | |
|--|--------|------------------------------------|----------------------------------|------------------------------------|----------------------------------|
| range of q | number | strictly gravitational orbits | | NG orbits | |
| | | $\langle 1/a_{\text{ori}} \rangle$ | $\langle q_{\text{ori}} \rangle$ | $\langle 1/a_{\text{ori}} \rangle$ | $\langle q_{\text{ori}} \rangle$ |
| 0.00–1.00 | 12 | 0.00210388 | 0.7195 | 0.00213188 | 0.7194 |
| 0.50–1.00 | 11 | 0.00216729 | 0.7638 | 0.00218800 | 0.7638 |
| 1.00–2.50 | 7 | 0.00120854 | 1.5826 | 0.00126796 | 1.5825 |
| all | 19 | 0.00177402 | 1.0374 | 0.00181360 | 1.0374 |

future NG-orbits is also clearly visible. Within the whole sample of 50 comets only eight have $E_{\text{fut}} < 0$, however six of them are new comets (about 25% of sample I) and remaining two are Oort spike comets.

Deviations from the solid line given in the bottom panel of Fig. 6 show how strongly the NG-effects change the cumulative planetary perturbations during the comet's passage through the solar system. The values of these deviations are mostly inside the range $-300 \cdot 10^{-6} \text{ AU}^{-1} < (E_{\text{fut}} - E_{\text{ori}})_{\text{NG}} - (E_{\text{fut}} - E_{\text{ori}})_{\text{GR}} < 300 \cdot 10^{-6} \text{ AU}^{-1}$, except three comets with labels in the bottom panel of Fig. 6. The mean value of $| (E_{\text{fut}} - E_{\text{ori}})_{\text{NG}} - (E_{\text{fut}} - E_{\text{ori}})_{\text{GR}} |$ is equal to $107 \cdot 10^{-6} \text{ AU}^{-1}$. Since the orbital periods of LP comets are much longer than those of perturbing planets it is usually assumed that LP comets are subjected to random change of energy during their passage through the solar system. Thus the Gaussian distribution adequately describes the $\delta E = E_{\text{fut}} - E_{\text{ori}}$ distribution. The standard deviation, σ , calculated from the best fitted Gaussian distribution of δE to the first quality orbits is $517 \cdot 10^{-6} \text{ AU}^{-1}$ (sample A+B; Table 1) and is $624 \cdot 10^{-6} \text{ AU}^{-1}$ for the first and second quality orbits (375 comets). Both values are smaller than the adopted value of $\sigma = 666 \cdot 10^{-6} \text{ AU}^{-1}$ given by Yabushita (1979) on the basis of various q values published earlier. Summarizing, the average error of approximately 20% in the value of planetary perturbations should be expected for individual comet due to omission the NG-effects.

In Table 2 the median and mean values of ΔE_{ori} and ΔE_{fut} are given for three basic samples of LP-comets. One can see that the median values (Model M1 in the table) as well as the mean values (Model M2) are greatest for the new comets (sample I), as compared to the 'Oort spike' and the 'old' comets (samples II and III). The mean values are systematically greater than the median values. Since ΔE_{ori} as well as ΔE_{fut} have significant scatter the median values seem to be more representative than the mean values for the typical variations of ΔE_{ori} and ΔE_{fut} due to NG-effects. The same is true for Δq_{ori} discussed above. Corrections of ΔE_{ori} given in the Table 2 were applied to all new+Oort spike comets in the section 7 according to Model M1 based on the median values as well as Model M2 based on the mean values.

Fig 4 shows the sparse distribution of the original energy variation, ΔE_{ori} in function of perihelion distance q (top panel) and similar behaviour of Δq_{ori} versus q (bottom panel). The analogical spread distributions were noticed also for the future energy variations and future perihelion changes in function of q .

Though the analysis of the mean and median values of ΔE_{ori} are given for comets with the first class quality orbits, it is interesting to mention that among the 'new' comets with the second class quality orbits two objects, C/1975 X1 Sato and C/1955 O1 Honda, have very large values of ΔE_{ori} , far outside the interval given in Fig. 3. Both comets have very large $1/a_{\text{ori}} > 1000 \cdot 10^{-6} \text{ AU}^{-1}$ for the NG orbit in comparison to their negative value of strictly gravitational $1/a_{\text{ori}}$. It is interesting that both comets belong to a group of three objects (all with the second quality class orbits) with the most negative $1/a_{\text{ori,GR}}$ (less than $-500 \cdot 10^{-6} \text{ AU}^{-1}$) (Table 6). In a consequence their ΔE_{ori} are also extremely large, namely $\Delta E_{\text{ori}} \simeq 1860 \cdot 10^{-6} \text{ AU}^{-1}$ for C/1975 X1 and $\Delta E_{\text{ori}} \simeq 2480 \cdot 10^{-6} \text{ AU}^{-1}$ for C/1955 O1, whereas the values of ΔE_{ori} of the 50 comets with the first quality orbits are between -290 and $+500$ in units of $\cdot 10^{-6} \text{ AU}^{-1}$ (Fig. 3). Comet 1955 O1 Honda is additionally peculiar since its two distinct nuclei were reported by Roemer (1955) and by van Biesbroeck (1957). Based on their observations Sekanina (1979) concluded that this comet must have broken up at a large heliocentric distance long before its discovery. The second comet, C/1975 X1 Sato, with the largest negative $1/a_{\text{ori,GR}}$, is also peculiar due to its very small total absolute magnitude ($H_{10} \leq 10$) (Marsden, 1970) that placed this object among the intrinsically faintest LP comets. However both comets have quite ordinary NG accelerations.

Table 4: The average values of the original energy, $\langle E_{\text{ori}} \rangle$ for sample A (column 3) and sample AA (column 5) for comets divided according to their q values into 13 bins (crosses and black dots at the top panel in Fig. 7).

| sample A | | | | sample AA | | |
|--------------|--------|------------------------------------|----------------------------------|-----------|------------------------------------|----------------------------------|
| range of q | number | $\langle 1/a_{\text{ori}} \rangle$ | $\langle q_{\text{ori}} \rangle$ | number | $\langle 1/a_{\text{ori}} \rangle$ | $\langle q_{\text{ori}} \rangle$ |
| 0.00–0.50 | 9 | -0.00001379 | 0.2707 | 9 | 0.00000344 | 0.2849 |
| 0.25–0.75 | 10 | 0.00000232 | 0.4842 | 15 | 0.00000989 | 0.5039 |
| 0.50–1.00 | 10 | -0.00001252 | 0.8188 | 15 | 0.00001729 | 0.7699 |
| 0.75–1.25 | 14 | 0.00000433 | 1.0132 | 17 | 0.00002287 | 1.0232 |
| 1.00–1.50 | 18 | -0.00001080 | 1.2377 | 19 | -0.00000352 | 1.2125 |
| 1.25–1.75 | 21 | -0.00000551 | 1.4953 | 20 | 0.00000135 | 1.4955 |
| 1.50–2.00 | 14 | 0.00003018 | 1.6694 | 15 | 0.00003906 | 1.6876 |
| 2.00–3.00 | 14 | 0.00002380 | 2.3954 | 13 | 0.00002584 | 2.3942 |
| 3.00–4.00 | 23 | 0.00003380 | 3.3684 | 23 | 0.00003567 | 3.3683 |
| 4.00–5.00 | 16 | 0.00002787 | 4.4031 | 16 | 0.00002787 | 4.4031 |
| 5.00–6.00 | 14 | 0.00004020 | 5.5000 | 14 | 0.00004020 | 5.5000 |
| 6.00–7.00 | 6 | 0.00002835 | 6.3234 | 6 | 0.00002835 | 6.3234 |
| 7.00–10.00 | 7 | 0.00004073 | 8.1556 | 7 | 0.00004073 | 8.1556 |
| 0.00–0.50 | 37 | -0.00001199 | 0.8893 | 43 | 0.00000519 | 0.8640 |
| 0.50–1.00 | 94 | 0.00003188 | 4.0091 | 94 | 0.00003411 | 4.0041 |
| all | 131 | 0.00001949 | 3.1279 | 137 | 0.00002503 | 3.0185 |

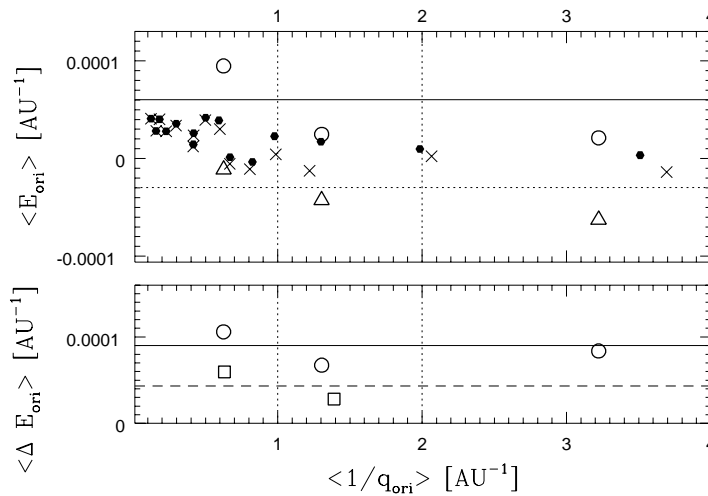


Figure 7: The average values of the original energy, $\langle E_{\text{ori}} \rangle$ (top panel) and the average value of the difference between the original energy of strictly gravitational orbit and the NG orbit $\langle \Delta E_{\text{ori}} \rangle$ (bottom panel) for comets divided according to their q values. Open circles and triangles correspond to the 'new' + Oort spike comets (sample I+II), whereas the open squares represent the 'old' comets (sample III; Table 3). Crosses in the top panel represent the mean values of $\langle E_{\text{ori}} \rangle$ for the sample of 131 comets of $\langle E_{\text{ori}} \rangle < 10^{-4} \text{ AU}^{-1}$ (sample A, Table 1) divided into 13 bins (Table 4), whereas the black dots show the same quantities for the sample of 137 comets (sample AA, Table 4).

6.1 Variations of the original semimajor axes with perihelion distance

Marsden et al. (1973) have shown that the mean of $1/a_{\text{ori}}$ of 'new' comets tend to be negative at small perihelion distance. They examined the sample of 61 class I comets (i.e. comets with well-determined orbits), and concluded that presumably this is due to the influence of the NG effects.

Here, I examine this problem on the basis of 56 comets with the detectable NG effects. To determine the average values of the reciprocals of the original semimajor axes, $E_{\text{ori,NG}} = 1/a_{\text{ori,NG}}$ and $E_{\text{ori,GR}} = 1/a_{\text{ori,GR}}$, the two subgroups were constructed, first consists of objects with $1/a_{\text{ori}} < 10^{-4} \text{ AU}^{-1}$ (sample I+II) and second – objects with $1/a_{\text{ori}} > 10^{-4} \text{ AU}^{-1}$ (sample III). The sample I+II was divided onto three subgroups containing 5 comets ($q < 0.5 \text{ AU}$), 10 comets ($0.5 \text{ AU} < q < 1.0 \text{ AU}$) and 16 comets ($q > 1.0 \text{ AU}$), respectively.

Sample III of 'old' comets contains only one object of $q < 0.5 \text{ AU}$. So it was practical to divide this sample on two subgroups only, with $q < 1.0 \text{ AU}$ (12 objects) and $q > 1.0 \text{ AU}$ (7 objects), respectively.

The average values of the original energy, $\langle E_{\text{ori,NG}} \rangle$ and $\langle E_{\text{ori,GR}} \rangle$ for comets divided according to their q values are given in Table 3, whereas the top panel of Fig. 7 shows these average values versus the average $1/q_{\text{ori}}$. These values based on the samples of comets with the detectable NG effects could be compared with the complete sample of 131 comets of $E_{\text{ori}} < 10^{-4} \text{ AU}^{-1}$ extracted from the MW Catalogue. Table 4 gives the average values of $\langle E_{\text{ori,GR}} \rangle$ for 13 overlapping groups of the sample A, and the crosses in the top panel of Fig. 7 show their distribution vs. reciprocals of q .

The impact of the NG effects on the E_{ori} of comets in the sample A is now assessed. First, the NG orbits derived for 31 comets of sample I+II were inserted instead of the strictly gravitational orbits taken from the MW Catalogue. Next, 11 gravitational first class orbits of comets with the indeterminable NG effects were taken instead the catalogue orbits. Thus, the new orbits were implemented for 42 comets, where 13 of them belonged to the comets outside the sample A (originally the comets having NG orbits in the MW Catalogue were ejected from the sample A). On the other hand, seven comets belonging to the sample A have NG orbits with $E_{\text{ori,NG}}$ greater than 10^{-4} AU^{-1} . Finally, the new corrected sample of comets with $E_{\text{ori}} < 10^{-4} \text{ AU}^{-1}$ (designed as the sample AA; Table 1) contains 137 objects, including 27 with the NG orbits. The average values of $\langle E_{\text{ori}} \rangle$ for thirteen overlapping groups of this sample are given in the column 6 of Table 4, and are shown as black dots at the top panel of Fig. 7. One can see that, the average values of E_{ori} have smaller dispersion than the respective values in the sample A. These dots could be compared to the open triangles inside the same q ranges. Among the sample I+II 74% of objects have $E_{\text{ori,GR}} < 10^{-5} \text{ AU}^{-1}$, whereas the sample AA includes less than 25% of such comets. In a consequence, the triangles are situated below the respective dots. The behaviour of $\langle E_{\text{ori}} \rangle$ as a function of $\langle 1/q_{\text{ori}} \rangle$ differs from the linear relation derived for 61 comets of class I by Marsden et al. (1973).

It is clearly visible that the average E_{ori} in the $1/q$ intervals for $q < 1.5 \text{ AU}$ are systematically smaller than for $q > 1.5 \text{ AU}$. The original energies $\langle E_{\text{ori}} \rangle$ for the low q orbits cluster around $+5 \cdot 10^{-6} \text{ AU}^{-1}$, while the large q orbits concentrate around $+34 \cdot 10^{-6} \text{ AU}^{-1}$ (Table 4, Fig. 7). The difference of $\sim 40 \cdot 10^{-6} \text{ AU}^{-1}$ between $\langle E_{\text{ori}} \rangle$ for these two intervals of q is smaller than the mean changes of the original energy between the NG-orbit and strictly gravitational orbit $\langle \Delta E_{\text{ori}} \rangle$ represented by open circles and solid horizontal line in the bottom panel of Fig. 7. Thus the tendency of the negative mean value of E_{ori} at small q for the sample of the 'new' and Oort spike comets (sample AA) would be canceled by the correct modification of known gravitational orbit due to NG-forces.

7 The Oort spike modification due to NG force

The sample AA of 137 comets contains 27 NG-orbits. Among the remaining 110 objects, 53 comets have perihelion distance $q > 3.1 \text{ AU}$. This value of q was assumed as the limiting distance for activity of the NG forces. Thus, for 68 comets with strictly gravitational orbits and $q < 3.1 \text{ AU}$ the $1/a$ -corrections given in the Table 3 according to Model M1 and Model M2 were applied. The resulting distributions of E_{ori} are given in the middle and bottom panel of Fig. 8, respectively.

I first discuss the model M2 based on mean values of ΔE_{ori} that gives greater corrections to the original semimajor axes. The Oort spike in the model M2 splits in two populations. This is because the $1/a$ -corrections have been applied only for $q < 3.1 \text{ AU}$. The left peak is centered around the value of $E_{\text{ori}} \sim 3 - 4 \cdot 10^{-5} \text{ AU}^{-1}$, slightly to the right from the old position of the observed Oort spike for strictly gravitational original energy. The newly formed right maximum peaks around the value $E_{\text{ori}} \sim 9 \cdot 10^{-5} \text{ AU}^{-1}$. The first is formed mostly by LP comets with great perihelion distances, whereas the latter – by comets with q below 3.1 AU. Almost 60% of comets with $q > 3.1 \text{ AU}$ have the original energy in the range $0 < E_{\text{ori}} < 7 \cdot 10^{-5} \text{ AU}^{-1}$, whereas only 5% of comets with $q > 3.1 \text{ AU}$ are in the range $7 \cdot 10^{-5} \text{ AU}^{-1} < E_{\text{ori}} < 12 \cdot 10^{-4} \text{ AU}^{-1}$ (see the inset in the bottom panel of Fig. 8). This double-peaked distribution for comets with $E_{\text{ori}} < 10^{-4} \text{ AU}^{-1}$ seems very attractive for theoretical modeling of long-term dynamical evolution of nearly parabolic comets.

Probably more realistic and more conservative seems Model M1 based on the median values of ΔE_{ori} . In this model the Oort spike is transformed into significantly more spread and less peaked distribution that is well represented by a gaussian distribution with the maximum at $E_{\text{ori}} = 5.5 \cdot 10^{-5} \text{ AU}^{-1}$ and $\sigma = 3.8 \cdot 10^{-5} \text{ AU}^{-1}$. Though the whole sample exhibits the normal distribution of E_{ori} , some traces of two populations are revealed when distributions of $1/a$ are plotted separately for comets with small and large q . Similarly to Model M2, also

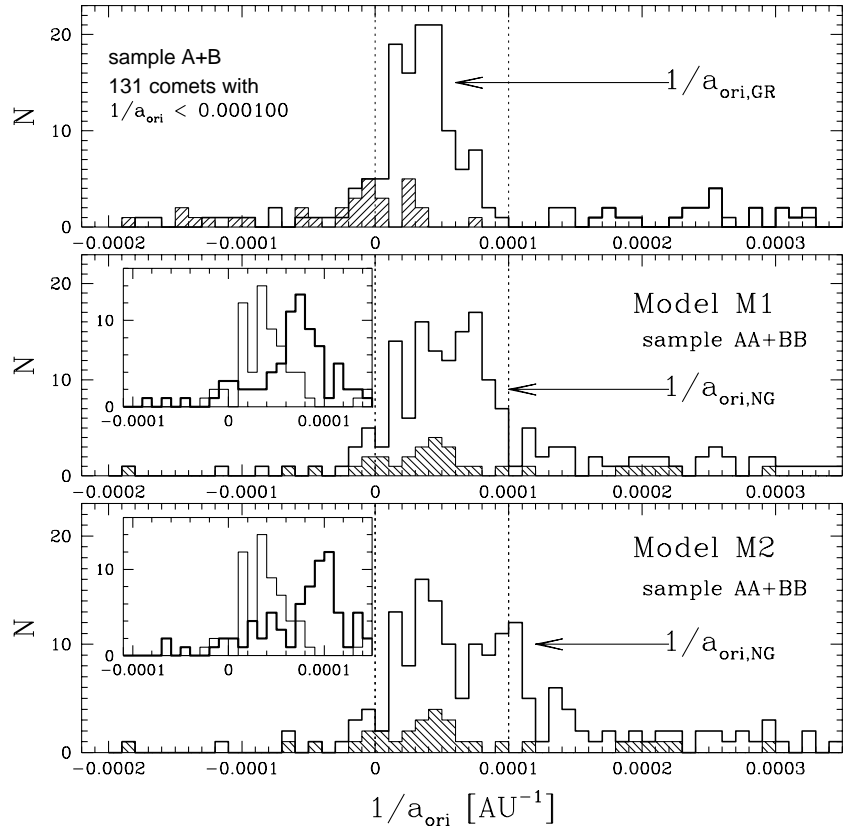


Figure 8: Top panel: The strictly gravitational Oort spike distribution, $E_{\text{ori,GR}}$ for the sample A (solid line histogram) and the distribution of $E_{\text{ori,GR}}$ for the basic sample I+II (shaded histogram). Middle and bottom panels: The Oort spike distributions (thick solid lines) corrected for the NG-effects according to Model M1 and Model M2, respectively, where corrections were applied to comets with $q < 3.1$ AU. The shaded areas at both lower panels represent the distribution of $E_{\text{ori,NG}}$ for the basic sample I+II. The insets show the respective distributions for comets with $q < 3.1$ AU (thick solid line), and comets with $q > 3.1$ AU (thin solid line), separately.

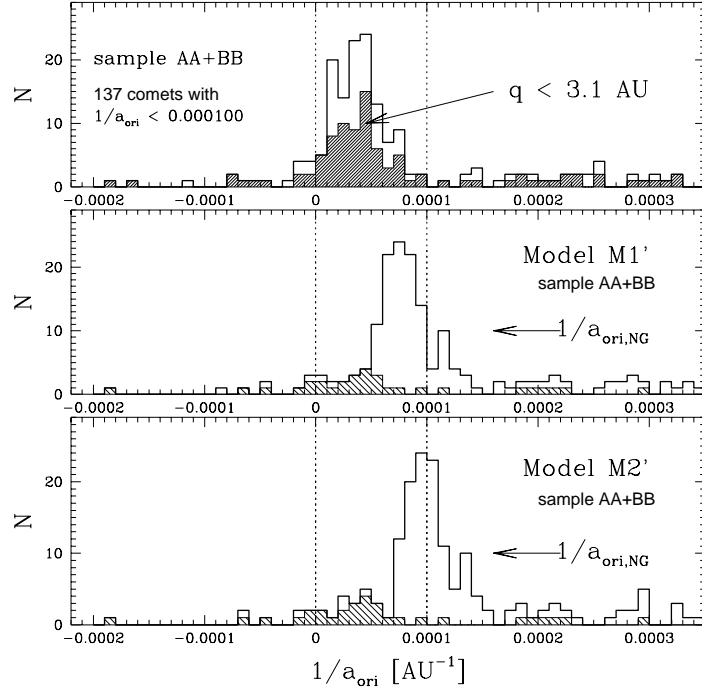


Figure 9: Top panel: The Oort spike distribution of comet energies for the sample AA (thick solid line), where the shaded distribution represents the comets with $q < 3.1$ AU. Middle and bottom panels: the same as in Fig. 8 where all the comets of sample AA were corrected for the NG-effects according to Model M1 and Model M2, respectively.

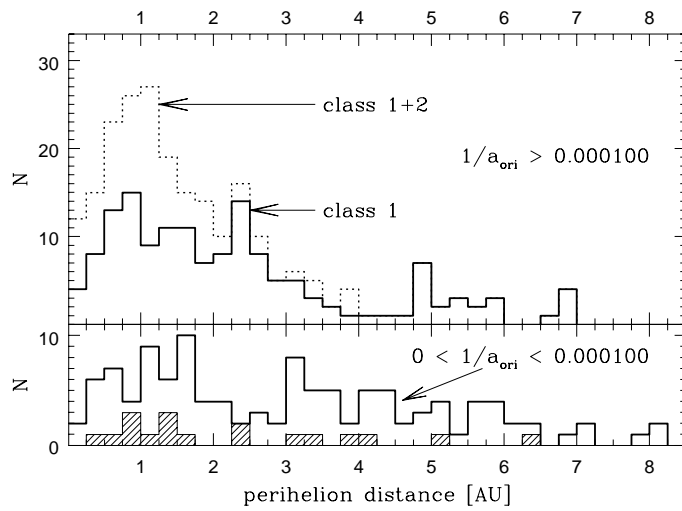


Figure 10: Comparison between distributions of perihelions of 'old' comets collected in sample BB (top panel, solid line histogram) and comets of sample AA (bottom panel). The sample AA is divided into hyperbolic (shaded histogram), and new + Oort spike comets (solid line distribution). The dotted line histogram in the top panel represents the distribution of comets with orbits of quality classes 1 and 2.

here the comets with large q dominate on the left-half of the range $0 < E_{\text{ori}} < 10^{-4} \text{ AU}^{-1}$, while the comets with small q are grouped mostly in the right-half of the same range. Inset given in the middle panel of Fig. 8 shows the respective histograms for $q < 3.1 \text{ AU}$ (thick solid line) and $q > 3.1 \text{ AU}$ (thin solid line).

Modifications of the Oort spike generated by the improved $1/a$ -corrections applied to all the comets are presented in the Fig. 9. The Oort spike is now shifted towards more positive energies than in the Fig. 8. The mean value of E_{ori} for the Oort spike is now centered roughly on $E_{\text{ori}} \simeq 7 - 8 \cdot 10^{-5} \text{ AU}^{-1}$ (middle panel) for the median corrections and $E_{\text{ori}} \simeq 9 - 10 \cdot 10^{-5} \text{ AU}^{-1}$ for the mean corrections (bottom panel).

8 Perihelion distance distributions of dynamically new and old comets

The problem of the actual perihelion distributions of the LP comets is complex due to various observational biases. The most severe effects are present in the old samples of LP comets because the data are highly incomplete beyond 1.5–2.5 AU. Recently, Hughes (2001) has shown that old discoveries of the LP comets (before ~ 1900) give a maximum around 0.8 AU. He derived that the maximum shifts to $\sim 1 \text{ AU}$ for comets discovered between 1987–1946, whereas the distribution of the LP comets detected after 1950 is significantly broader and peaks between 1–2 AU. He also concluded that modern cometary catalogues of the LP comets are still incomplete beyond 2.5 AU. To derive the true perihelion distribution for the active LP comets at large q it is necessary to introduce the corrections for the observational bias in the comet discoveries. At present such corrections are not available and the distributions discussed here are also subject to this bias.

The upper panel in Fig. 10 shows the observed perihelion distributions of the 'old' comets of class 1 (sample BB, solid line histogram) and class 1+2 (dotted line histogram), separately. The observed perihelion distributions of 'new' + Oort spike comets (sample AA without hyperbolic comets) is presented in the bottom panel of Fig. 10. One can see the significant differences between both histograms of comets with the first class orbit. It is well-known that the perihelion distribution of the LP comets has a maximum near $q \approx 1 \text{ AU}$. This also results from the observational selection. The theoretical modeling of the cometary dynamics suggests that the actual number of comets per unit perihelion distance increases with increasing q (Weissman, 1985). However, probability of the comet detection diminishes with the increasing distance from the Sun and Earth. In effect, the observed distribution of the LP comets is peaked near $q = 1 \text{ AU}$ from the Sun. The distribution of the 'old' LP comets (class 1+2, dotted line histogram in the top panel of Fig. 10) reflects exactly the same effect.

In contrast to the 'old' LP comets, the perihelion distributions of the 'new' and Oort spike comets with $0 < E_{\text{ori}} < 1 \cdot 10^{-4} \text{ AU}^{-1}$ are quite different (thick-line histogram in the bottom panel of Fig. 10). The numbers of objects in the consecutive perihelion distance bins are 19 (0–1 AU), 29 (1–2 AU), 11 (2–3 AU), 20 (3–4 AU), 15 (4–5 AU), and 25 for $q > 5 \text{ AU}$ (21%). This gives 50% of objects with perihelions inside sphere of 3 AU for the new and Oort spike comets, while fraction of the 'old' comets with $q < 3 \text{ AU}$ reaches 76%. A relative excess of the 'new' and Oort spike comets with the large perihelion distance over the 'old' comets result – at least to some extent – from the efficient processes of the gradual decline of activity during the cometary evolutions. It is well known that to obtain the agreement between the observed distribution of original cometary energy and the expected one by theory some fading model must be assumed (Weissman, 1980; Bailey, 1984; Wiegert & Tremaine, 1999). However, such modeling of fading is complicated by a fact that dynamically new comets are often anomalously bright at large perihelion distances (especially on the inbound leg of their orbits), probably due to sublimation of more volatile ices than water (and possibly larger sizes of the cometary nuclei). The observed q distribution of the 'new' and Oort spike comets (thick-line histogram in the bottom panel of Fig. 10) could be represented either by a single-peaked distribution with broad maximum somewhere between 1–4 AU or by double-peaked distribution consisting of two populations, where the left-hand peak has the same interpretation as in the case of the entire sample of 'LP' comets. These comets sublimate mostly the water ice. A merged sample of hyperbolic comets (shaded histogram in the bottom panel of Fig. 10) and the 'new' and Oort spike comets (thick line histogram) has a broad main maximum centered at 1 AU. Nevertheless, the local maximum for perihelions greater than 3 AU or local minimum within $1.75 \text{ AU} < q < 3.00 \text{ AU}$ is still perceptible. Orbits within this local minimum are mostly retrograde and this fact will be discussed in the next section.

9 Distributions of prograde and retrograde orbits

Fernandez (2002) divided the observed population of the LP comets into 8 subgroups according to the original orbital energy E_{ori} . He found that distributions of Oort spike comets with $23.8 \cdot 10^{-6} \text{ AU}^{-1} < E_{\text{ori}} < 100 \cdot 10^{-6} \text{ AU}^{-1}$ (three groups) show excess of the retrograde orbits, while the remaining groups show a weak excess of direct orbits. He argued that this excess of retrograde orbits is connected with the higher probability of diffusing through the Jupiter-Saturn barrier for comets in the retrograde orbits than for comets in the direct orbits. I have performed a similar analysis for the corrected global samples AA and BB dividing the first of them into two subgroups and the second – into 3 subgroups. Within two subgroups of the 'new' + Oort spike comets no excess has been obtained. The whole sample AA contains almost the same number of comets on direct orbits (71 objects) as on retrograde orbits

Table 5: Distributions of direct and retrograde orbits for three samples of the LP comets with perihelions between 1.75 AU and 3.00 AU

| range of q | Sample AA | | Sample BB | | Sample AA+BB | |
|--------------|----------------|----------------|----------------|----------------|----------------|----------------|
| | $i < 90^\circ$ | $i > 90^\circ$ | $i < 90^\circ$ | $i > 90^\circ$ | $i < 90^\circ$ | $i > 90^\circ$ |
| 1.75–2.25 | 0 | 8 | 7 | 7 | 7 | 15 |
| 2.25–3.00 | 3 | 6 | 10 | 18 | 13 | 24 |
| 1.75–3.00 | 3 | 14 | 17 | 25 | 20 | 39 |

(65 objects). A small excess of retrograde orbits was obtained for the sample of all the 'old' comets (sample BB): 82 of 149 move on retrograde orbits. However, among three subgroups of the 'old' comets only one of them, defined by $100 \cdot 10^{-6} \text{ AU}^{-1} < E_{\text{ori}} < 500 \cdot 10^{-6} \text{ AU}^{-1}$, shows statistically significant excess of the retrograde orbits (34 comets) in comparison to the direct orbits (12 comets). This sub-sample corresponds to the sub-sample 'e' constructed by Fernandez (2002), for which the most prominent excess of retrograde orbits is visible in the Fig. 1 of his paper. Very similar results were derived when the sample of 286 comets with the first class orbits (sample AA+BB) were supplemented by 113 comets with the second class orbits. Then, like previously, among five sub-samples only this define by $100 \cdot 10^{-6} \text{ AU}^{-1} < E_{\text{ori}} < 500 \cdot 10^{-6} \text{ AU}^{-1}$, shows statistically significant excess of the retrograde orbits (41 comets) in comparison to the direct orbits (16 comets).

The significant excess of the retrograde orbits was also found for the LP comets having $1.75 \text{ AU} < q < 3.00 \text{ AU}$. Table 5 shows that such excess is evident in both corrected samples of LP comets. However, among the 'new' and Oort spike comets (sample AA) the number of the retrograde orbits exceeds four times the number of the direct orbits, whereas within the old comets – the excess amounts to 50%. One should note, that among ten dynamically new comets having perihelions between 1.75 AU and 2.25 AU all move on the retrograde orbits. In the q range of $1.75 \text{ AU} < q < 3.00 \text{ AU}$ the local deficiency of the 'new' + Oort spike comets is observed (see Fig. 10), while the perihelion distribution of the 'old' comets has local maximum at $2.25 \text{ AU} < q < 2.75 \text{ AU}$. It seems that some mechanism prevents the 'new' and Oort spike comets entering the solar system on the direct orbits to reach this range of the perihelion distances. Apparently this bias does not affect strongly the retrograde orbits. It is likely that the 'old' comets are also subject to the same mechanism.

10 Summary and concluding remarks

In the present study the NG effects are derived for 50 LP comets, where 31 of them have $E_{\text{ori,GR}} < 10^{-4} \text{ AU}^{-1}$. It was confirmed that NG forces make 'hyperbolic' and elliptical osculating orbits less eccentric than by assuming purely gravitational motion. Such number of comets with the detectable NG effects allow us to give some estimates of the average value of $\Delta E_{\text{ori}} = 1/a_{\text{ori,NG}} - 1/a_{\text{ori,GR}}$ for three subsamples of the LP comets. Due to large dispersion of the ΔE_{ori} distributions (within each subsample) the median values of ΔE_{ori} seem to represent more adequately typical corrections for $E_{\text{ori,GR}}$ of the LP comets with the non-detectable NG effects.

Applying these corrections for the all LP comets, the estimates of the Oort spike shift from its classical position (i.e. position derived on the basis of pure gravitational model of comet's motion) have been obtained.

Unfortunately, the available data warrant only simplified type of models of the $1/a$ corrections. In the first type it was assumed that the NG effect are present only for $q < 3.1 \text{ AU}$ (Fig. 8), while in the second type no upper limit for q was imposed (Fig. 9). Although one could expect smooth decline of the NG effects with the increase of the perihelion distance, no such relationship is implied by the observational data. In particular it is not present in the our basic sample of 50 comets (the bottom panel in Fig. 7 and section 6.1). On the other hand, the active comets at large perihelion distances have been observed (e.g. C/2004 T3 Siding Spring with $q = 8.9 \text{ AU}$, C/2000 A1 Montani with $q = 9.7 \text{ AU}$, and C/2003 A2 Gleason with $q = 11.4 \text{ AU}$). In such cases another formula for the NG acceleration due to sublimation of more volatile ices is necessary. Such modeling of the NG effects in the LP comets with large perihelion distance based on Yabushita CO-function (Yabushita, 1996) was performed in Paper II. However, no reliable NG effects have been found for comets with the perihelion distance greater than 3.5 AU.

Using the model of the NG effects limited to comets with $q \leq 3.1 \text{ AU}$, the Oort spike is transformed into significantly more spread and less peaked distribution with the maximum at $E_{\text{ori,NG}} = 5.5 \cdot 10^{-5} \text{ AU}^{-1}$, whereas if no upper limit on q is imposed the Oort spike peaks near $E_{\text{ori,NG}} \simeq 8.5 \cdot 10^{-5} \text{ AU}^{-1}$ (middle panels of Figs. 8 and 9). Assuming conservatively $E_{\text{ori,NG}} = 5.5 \cdot 10^{-5} \text{ AU}^{-1}$ the outer Oort Cloud distance from the Sun is approximately 37 000 AU. Consequently the inner edge of the Oort Cloud is situated at a distance significantly smaller than the 'classical' 20 000 AU assumed in the literature. The middle panel of Fig. 8 suggests that this inner edge could be less spectacular than in the classical point of view, i.e. in the strictly gravitational case (top panel of Fig. 8).

On the other hand, the theoretical simulations predict that the energies of new comets should peak near $E_{\text{ori}} \approx 2.9 \cdot 10^{-5} \text{ AU}^{-1}$, i.e. at a semimajor axis of about 34 000 AU for the currently accepted value of a local mass density of $0.1 \text{ M}_\odot/\text{pc}^3$ (Levison et al., 2001). Assuming that Sun formed in a denser galactic environment than it occupies now, it is possible to obtained the Oort Cloud bound more tightly (Eggers, 1999; Fernandez, 2002). For example, taking an initial local density of 100 times greater than the current local density, and assuming that

the early Sun spent in such environment first 20 m.y. yrs, Eggers (1999) modeled the Oort cloud formation. She has found that the tightly bound cloud of comets might have been formed at a heliocentric distance of about 6–7 thousand AU.

It is obvious that such significant reduction of the Oort cloud distance as postulated in the present paper has a deep consequences in many aspects of theoretical modeling of the Oort Cloud formation as well as simulations of a long-term evolution of the Oort Cloud comets, and cometary fading and disruption. In the last decades, all these three blocks of issues have been intensively explored (see reviews by Dones et al. (2004), and Rickman (2004)). However, evolutionary correlations between the observed cometary populations and their reservoirs are still incomplete and are inconsistent in many aspects (Emel'yanenko & Bailey, 1998; Nurmi et al., 2002; Rickman, 2005) One of the most important problems raised by the recent simulations (Levison et al., 2001; Duncan et al., 1987; Dones et al., 2004) are correlations between the outer and inner Oort Cloud populations and their characteristics. Still more realistic simulations are needed.

References

Bailey, M.E., 1984, MNRAS, 211, 347
 van Biesbroeck, G., 1957, AJ, 62, 191
 Dones, L., Weissman, P.R., Levison, H.F., & Duncan, M.J., 2004, Oort Cloud Formation and Dynamics, in Comets II, ed. M.C. Festou H.U. Keller, & H.A. Weaver (University of Arizona, Tucson), 153
 Duncan, M., Quinn, T., & Tremaine, S., 1987, AJ, 94, 1330
 Dybczynski, P.A., 2005, AA 441, 783
 Emel'yanenko, V.V., & Bailey, M.E., 1998, MNRAS, 298, 212
 Eggers, S., 1999, Ph.D. thesis, Max Planck Institut für Aeronomie, Katlenburg-Lindau, Germany
 Fernandez, J.A., 2002, Proceedings of Asteroids, Comets, Meteors ACM 2002, ESA SP-500, 303
 Fernandez, J.A., & Brunini, A., 2000, Icarus 145, 580
 Heisler, J., 1990, Icarus, 88, 104
 Hughes, D.W., 1991, J. Br. Astron. Assoc., 101, 119
 Hughes, D.W., 2001, MNRAS 326, 515
 Królikowska, M., 2001, A&A, 376, 316 (Paper I)
 Królikowska, M., 2004, A&A, 427, 1117 (Paper II)
 Levison, H.F., Dones, L., & Duncan, M.J., 2001, AJ, 121, 2253
 Marsden, B.G., 1970, IAU Circ. No 2884
 Marsden, B.G. and Sekanina Z., 1973, AJ, 78, 1118
 Marsden, B.G., Sekanina Z., & Yeomans, D.K., 1973, AJ, 78, 211
 Marsden, B.G., Sekanina Z., & Everhart, E., 1978, AJ, 83, 64
 Marsden, B.G., Williams, G.V., 2005, Catalogue of Cometary Orbits, Sixteenth ed. (MW Catalogue)
 Nurmi, P., Valtonen, M.J., Zheng, J.Q., & Rickman, H., 2002, MNRAS, 333, 835
 Oort, J.H., 1950, Bull. Astron. Inst. Neth., 11, 91
 Rickman, H., 2004, Current Questions in Cometary Dynamics, in Comets II, ed. M.C. Festou H.U. Keller, & H.A. Weaver (University of Arizona, Tucson), 205
 Rickman, H., 2005, Transport of comets to the Inner Solar System, Proceedings of Dynamics of Populations of Planetary Systems, ed. Z. Knezevic, & A. Milani, 277
 Roemer, E., 1955, PASP, 67, 424
 Sekanina, Z., 1979, Icarus, 38, 300
 Sen, A.K., & Rana, N.C., 1993, A& A, 275, 298
 Sitarski G., 1989, Acta Astron., 39, 345
 Sitarski G., 2002, Acta Astron., 52, 471
 Weissman P.R., 1980, A& A 85, 181.
 Weissman, P.R., 1985, in Dynamics of Comets: Their Origin and Evolution, ed: Carusi A., and Valsecchi, IAU Colloquium 83, Reidel, Dordrecht, 87
 Wiegert, P., & Tremaine, S., 1999, Icarus, 137, 84
 Yabushita, S., 1979, MNRAS, 187, 445
 Yabushita, S., 1996, MNRAS, 283, 347

Table 6: Original and future reciprocals of semimajor axes derived in the present investigations for the sample of comets with $1/a_{\text{ori}}$ (obtained using the catalogue orbits): below 10^{-5} AU (part (i) & (ii) of this table), $10^{-5} \text{ AU} < 1/a_{\text{ori}} < 10^{-4}$ AU (part (iii)), and $1/a_{\text{ori}} > 10^{-4}$ AU (part (iv)) In the columns 2–6 the perihelion distance, the observational arc and number of observations taken for orbit determinations, orbit's quality class and the sample designation are given. Remarks in the last column denote: pp – present paper; PIgr – only strictly gravitational model in Paper I; PIdif – different selection than in Paper I; PImore – more observations than in Paper I; PaperI, PaperII – solutions taken from Paper I and Paper II, respectively.

| Name | q [AU] | Observational interval | Number of obs. | class MW Cat. | Sample | $1/a_{\text{ori}}$ | | $1/a_{\text{fut}}$ | | Remarks |
|--|-----------|---------------------------|-------------------|---------------------|--------|--------------------|---------------------------------------|--------------------|--------------|---------|
| | | | | | | grav | [in units of 10^6 AU^{-1}] | NG | grav | |
| (i) Long period comets of $1/a_{\text{ori}} < 10^{-5} \text{ AU}^{-1}$ obtained using the MW Catalogue orbits | | | | | | | | | | |
| C/1895 W1 | 0.192 | 18951118–18960810 | 114 | 1B | I | −146.0±13.5 | +201.1±280.4 | +482.4±13.5 | +430.1±34.0 | pp |
| C/1975 V2 | 0.219 | 19751113–19760209 | 85 | 2A | – | −138.8±25.5 | +358.0±153.6 | +1135±26 | +880.3±122.9 | PIdif |
| C/1911 S3 | 0.303 | 19110929–19120217 | 287 | 2A | – | −160.7±42.9 | −457.5±260.3 | +88.4±42.9 | +578.4±315.2 | pp |
| C/1899 E1 | 0.327 | 18990305–18990811 | 305 | 1B | I | −54.9±12.5 | −189.2±61.3 | −1199±13 | −1078±38 | PIgr |
| C/1940 R2 | 0.368 | 19400825–19410401 | 370 | 1B | I | −29.6±26.3 | +44.0±33.8 | −1600±26 | −1386±59 | pp |
| C/1991 Y1 | 0.644 | 19911224–19920502 | 274 | 1B | I | −97.3±8.8 | −60.2±10.3 | +1111±9 | +1148±10 | PIdif |
| C/2002 O4 | 0.776 | 20020727–20021001 | 1223 | 2A | – | −835.2±19.6 | −692.5±62.4 | −371.3±19.6 | +29.4±49.1 | pp |
| C/1952 W1 | 0.778 | 19521210–19530718 | 36 | 1B | I | −140.9±22.2 | −1.1±84.7 | −298.8±22.2 | −42.3±108.9 | PIgr |
| C/1975 X1 | 0.864 | 19751209–19760204 | 82 | 2B | – | −1053.5±243 | +805.1±573.4 | −1781.5±243 | 77.3±573.5 | PIdif |
| C/1955 O1 | 0.885 | 19550802–19551112 | 65 | 2A | – | −584.2±15.2 | +1892.5±380 | −289.0±15.2 | +1839±348 | PImore |
| C/1996 N1 | 0.926 | 19960704–19961103 | 316 | 1B | AA | −156.7±6.9 | – | +530.1±6.9 | – | PIdif |
| C/1993 Q1 | 0.967 | 19930816–19940417 | 526 | 1A | I | −1.1±3.4 | −5.4±8.6 | −70.1±3.4 | −223.0±38.6 | pp |
| C/1892 Q1 | 0.976 | 18920901–18930713 | 228 | 1B | I | −58.6±12.7 | +31.7±19.3 | −570.0±12.7 | −478.6±19.3 | PIgr |
| C/1896 V1 | 1.063 | 18961103–18970430 | 91 | 1B | AA | +0.5±33.0 | – | −804.1±33.0 | – | pp |
| C/1996 J1B | 1.298 | 19960510–19981217 | 529 | 1A | I | −1.4±2.0 | −10.4±15.7 | +568.0±2.0 | +603.8±2.4 | PIgr |
| C/1996 E1 | 1.359 | 19960315–19961012 | 249 | 1A | I | −43.3±4.2 | +28.1±11.5 | +355.0±4.2 | +343.0±31.3 | PaperII |
| C/1932 M1 | 1.647 | 19320621–19330120 | 187 | 1B | AA | −19.1±24.7 | – | −250.9±24.7 | – | PImore |
| C/1946 C1 | 1.724 | 19460129–19470809 | 498 | 1A | I | −13.1±5.3 | +92.1±19.8 | +373.0±5.3 | +335.6±9.4 | PIdif |
| C/1978 R3 | 1.772 | 19780914–19790925 | 52 | 1B | AA | +67.6±32.9 | – | +283.7±32.9 | – | pp |
| C/1983 O2 | 2.255 | 19830804–19840605 | 39 | 1B | AA | −16.1±20.9 | – | +403.8±20.9 | – | PaperI |
| C/1898 V1 | 2.285 | 18981115–18990604 | 71 | 1B | AA | −14.1±59.5 | – | +676.7±59.4 | – | PImore |
| C/1946 U1 | 2.408 | 19461101–19481002 | 143 | 1A | I | +2.7±6.7 | +192.1±33.0 | +29.5±6.7 | +12.2±10.5 | PIdif |
| C/1987 W3 | 3.333 | 19870924–19900429 | 34 | 1A | AA | +24.4±7.3 | – | −361.6±7.3 | – | pp |
| C/1997BA6 | 3.436 | 19970111–20040815 | 529 | 1A | I | −1.5±0.5 | +38.4±1.7 | +371.8±0.5 | +404.9±1.7 | PIgr |
| C/2002 R3 | 3.870 | 20020804–20031210 | 1268 | 1B | AA | +39.0±0.6 | – | +9.9±0.6 | – | pp |
| C/1942 C2 | 4.113 | 19420212–19430311 | 48 | 1A | AA | −26.6±14.7 | – | −275.8±14.7 | – | PIdif |
| C/2002 A3 | 5.151 | 20020113–20030624 | 291 | 1B | AA | +25.2±27.8 | – | +6179±28 | – | pp |
| C/1978 G2 | 6.283 | 19780412–19800123 | 7 | 1B | AA | −22.5±45.0 | – | −99.3±45.0 | – | PaperI |
| Oort spike comet for the Catalogue orbits; hyperbolic in the present paper | | | | | | | | | | pp |
| C/1991 X2 | 0.199 | 19911213–19920303 | 155 | 2B | – | −83.9±174.9 | −26.3±151.2 | −710.8±174.9 | −653.2±151.1 | pp |
| (ii) Long period comets with NG-effects in the MW Catalogue and $1/a_{\text{ori}} < 10^{-5} \text{ AU}^{-1}$ for orbit determined in the present paper | | | | | | | | | | |
| C/1956 R1 | 0.316 | 19561108–19580411 | 249 | NG orbit | I | −104.8±3.1 | +7.6±11.5 | −610.3±5.1 | −587.4±10.9 | PImore |
| C/1959 Y1 | 0.504 | 19600104–19600617 | 88 | NG orbit | I | −138.9±16.4 | +3.5±143.4 | −590.6±16.4 | −280.5±49.4 | PaperII |
| C/2002 T7 | 0.616 | 20021102–20050512 | 4408 | NG orbit | I | −24.7±0.3 | +16.6±0.4 | −664.4±0.3 | −653.3±1.1 | pp |
| C/1989 Q1 | 0.642 | 19890824–19891224 | 231 | NG orbit | I | −4.3±12.7 | +62.5±28.3 | +190.4±12.7 | +92.8±38.3 | PIdif |
| C/1885 X1 | 0.642 | 18851201–18860719 | 228 | NG orbit | I | +8.7±13.7 | +31.3±20.0 | −245.3±13.7 | −100.4±48.2 | pp |
| C/2001 Q4 | 0.961 | 20010824–20050826 | 2552 | NG orbit | I | +5.6±0.5 | +57.4±0.8 | −738.6±0.5 | −695.3±0.8 | pp |
| C/1995 Y1 | 1.055 | 19951226–19960921 | 262 | NG orbit | I | −19.6±6.3 | −46.4±14.9 | +532.1±6.3 | +645.1±10.7 | PaperII |
| C/1998 P1 | 1.147 | 19980811–19990515 | 461 | NG orbit | I | −125.1±10.1 | +211.1±11.1 | +1119±10 | +1320±8 | PaperII |
| C/1986 P1A | 1.200 | 19860805–19890411 | 688 | NG orbit | I | −0.4±1.0 | +42.4±2.4 | +725.2±1.0 | +767.6±2.8 | PaperII |
| C/1971 E1 | 1.233 | 19710309–19710909 | 138 | NG orbit | I | −182.0±72.4 | +296.0±128.9 | −527.8±72.4 | −97.8±71.6 | PIdif |
| C/1993 A1 | 1.938 | 19930102–19940610 | 746 | NG orbit | I | −19.3±3.9 | +57.9±2.7 | −539.3±3.9 | −408.6±5.3 | PaperII |
| (iii) Oort spike comets for the catalogue orbits | | | | | | | | | | |
| C/1989 X1 | 0.350 | 19891206–19900627 | 281 | 1A | II | +22.4±2.4 | +42.3±12.8 | −365.6±2.4 | −373.3±6.9 | pp |
| C/1990 K1 | 0.939 | 19900521–19920401 | 678 | NG orbit | II | +26.0±1.6 | +111.6±7.2 | −848.6±1.6 | −790.4±3.4 | PaperII |
| C/1915 C1 | 1.005 | 19150213–19160926 | 646 | NG orbit | II | +73.1±5.2 | +224.9±18.8 | +958.7±5.2 | +1042±9 | pp |
| C/2003 K4 | 1.024 | 20030528–20050903 | 3190 | 1A | II | +38.1±0.2 | +28.2±0.6 | −180.2±0.2 | −118.3±1.2 | pp |
| C/1913 Y1 | 1.106 | 19131218–19150907 | 1046 | 1A | II | +23.2±1.7 | +58.1±5.7 | +57.5±1.7 | +92.3±5.7 | pp |
| C/1978 H1 | 1.136 | 19780428–19791209 | 287 | 1A | II | +24.4±2.7 | +77.5±17.3 | −1028±3 | −1020±8 | pp |
| C/1947 Y1 | 1.500 | 19480110–19481130 | 124 | 1B | II | +27.3±1.1 | +181.1±49.6 | +52.7±1.1 | +30.8±12.9 | pp |
| C/1997 J2 | 3.051 | 19970505–19991009 | 1446 | 1B | II | +36.8±0.6 | +45.5±1.0 | −4.8±0.6 | +15.5±1.1 | PIgr |
| (iv) 'Old' comets with $1/a_{\text{ori}} > 10^{-4} \text{ AU}^{-1}$ for orbits determined in the present paper | | | | | | | | | | |
| C/1974 C1 | 0.503 | 19740214–19741118 | 198 | NG orbit | III | +697.2±12.4 | +563.9±68.8 | +710.3±12.5 | +785.8±16.1 | pp |
| C/2000 WM1 | 0.555 | 20001116–20021013 | 2206 | NG orbit | III | +518.3±0.4 | +535.4±1.2 | −247.6±0.4 | −227.6±1.3 | pp |
| C/1985 R1 | 0.695 | 19850913–19860319 | 173 | NG orbit | III | +564.5±3.6 | +595.2±20.9 | +231.7±5.6 | +288.1±17.9 | pp |
| C/2003 T4 | 0.850 | 20031013–20050512 | 908 | NG orbit | III | +231.5±3.5 | +321.6±1.9 | −764.4±3.5 | −169.0±1.7 | pp |
| C/1953 T1 | 0.970 | 19531116–19540628 | 59 | NG orbit | III | +204.6±17.7 | +147.8±23.3 | −830.5±17.4 | −688.6±23.3 | pp |
| C/2002 U2 | 1.209 | 20021025–20030522 | 416 | 1B | III | +1033±3 | +1214±53 | +676.0±3.0 | +715.0±5.3 | pp |
| C/1998 M5 | 1.742 | 19980630–20000508 | 1222 | 1A | III | +512.8±0.5 | +510.9±1.0 | +2612.5±0.4 | +2628±2 | pp |